Design of predictive control strategies for active BITES systems using frequency domain models

Yuxiang Chen[1,2,3]

Postdoctoral fellow

Andreas K. Athienitis[1,2,3]

Professor and Director

Khaled E. Gala[1]

Associate Professor

[1] Concordia University, Department of Building, Civil, and Environmental Engineering

Montreal, Quebec, Canada, H3G 1M8

[2] NSERC Smart Net-zero Energy Buildings Strategic Research Network

www.solarbuildings.ca

[3] Centre for Zero Energy Building Studies of Concordia University

http://czebs.encs.concordia.ca

ABSTRACT

Active building-integrated thermal energy storage (BITES) systems, such as ventilated concrete slabs, are able to effectively store and release abundant of thermal energy to assist space conditioning. Since active BITES systems are strongly thermal-coupled to the rest of the room, the desires for comfortable room temperature and utilization of renewable thermal energy, together with BITES' large thermal inertia place challenges in the operation of active BITES systems. With desired room temperature profiles and corresponding thermal loads, frequency domain models can readily provide predictive operation information for the active BITES systems. This paper will demonstrate the concept, methodology, and techniques in using frequency domain models to conduct predictive operations of active BITES systems. Using frequency domain models in optimizing the design of active BITES systems will also be discussed.

INTRODUCTION

To reduce the energy consumption and shave/shift peak demand of space conditioning (i.e. heating/cooling), integrated utilization of thermal energy storage and ambient renewable energy (e.g. solar heat and cool outdoor air) with proper design and control has proven promising, and attract significant interests of research and practice (Hadorn 2005). Building-integrated thermal energy storage (BITES), which uses building fabric (e.g. concrete slabs or masonry walls) as thermal storage mass, is among one of the effective measures (Braun 2003, Chen et al. 2010a). This measure, in contrast to conventional centralized and thermally isolated storage systems (e.g. water/ice tanks), avoids extra space occupation and material cost. Furthermore, BITES systems can effectively moderate the room temperature because their largely exposed surface enhances their thermal coupling with the rest of the room as shown in Figure 1. It has direct thermal interactions with room air by convection, with other room objects (e.g. other surfaces, furniture, and occupant pleasantly) by radiation. The systems shown in Figure 1 can be located in the ceiling, floor, or walls.
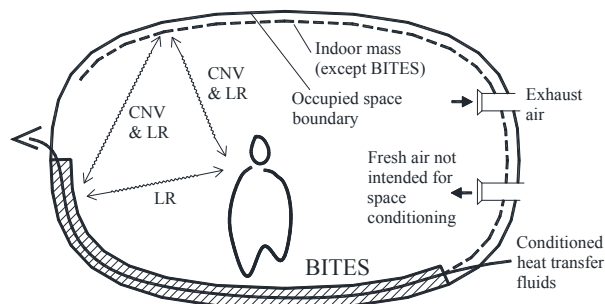

Figure 1. Schematics of a close-loop active BITES systems and thermal coupling with the interior space: ("Indoor mass" includes room air, wallboards, and furniture; CNV: convection; LR: long-wave radiation)

Active charge and/or discharge can be supplemented to traditional passive BITES systems (e.g. solid slabs) by adding core conditioning systems. These core conditioning systems can be hydronic, air-based (i.e. ventilated) or electric. Active charge and/or discharge enhance the engagement of core thermal mass for heat exchange by involving more heat exchange area. Hence, it increases the effective capacity of thermal storage and the heat exchange rate. This means more thermal energy can be stored in the BITES systems, and heat can be stored or extracted faster. In a close-loop system (Figure 1), the core conditioning systems can be hydronic or air-based. The thermal output from the BITES system to the rest of the room is through convection and long-wave radiation on the exposed surface of the BITES system, neglecting conduction at edges.

Even though active BITES systems have shown high potential in improving thermal and energy performance of buildings, challenges exist on their operation control (i.e. charge and/or discharge) and design due to following key factors:

(1) The thermal behavior of an active BITES system significantly influences the occupant thermal comfort due to its strong thermal coupling with the rest of the room.
(2) The high thermal inertia of BITES systems. This means slow response and significant amount of thermal energy is needed for temperature regulation. High power input intensity and relatively precise control are needed for fast regulation without overshooting (i.e. over-heating/-cooling).
(3) Improving building energy performance, such as
   a) Maximal utilization of ambient renewable energy to lower utility energy purchase.
   b) Pre-conditioning BITES with off-peak utility energy and shave peak demand;
   c) Allow or help room temperature to change along with exterior weather conditions to reduce the space conditioning load with smaller temperature difference between interior and exterior, or to use occupied space as thermal storage, and thermal collector as well is possible.

These factors are more challenging in cases that thermal energy released from active BITES systems provides the primary space conditioning (Figure 1), which is the focus of this study. After all, active BITES systems should be operated to satisfy thermal comfort requirement as their first priority. Upon achieving that, they should be utilized to improve the building energy performance to the most extent.

The ultimate control objective for active BITES systems is to conduct energy-efficient and economical operations that fulfill the thermal comfort requirement of occupants. This objective requires integrated design and control of the TES and space conditioning functions of active BITES systems. ASHRAE (2007) pointed out that the economic benefits of optimal but complicate strategies are not significant in comparison to basic and robust strategies that rely on simpler control routines.

Suitable room temperature, among other factors, is critical in satisfying thermal comfort requirement. Its profile bounds the operations of the active BITES system, and hence affects the energy performance. Therefore, a methodology using room temperature as leverage for the predictive control of the active BITES systems is developed in this study. The objective of this methodology is to satisfy the thermal comfort requirement on room temperature, as well as to enhance the building energy performance.

In addition to control, frequency domain models also provide insightful information for design optimization. The magnitude and phase angle of the transfer functions in frequency domain provide substantial insights of active BITES systems' thermal behavior (Athienitis 1994, Athienitis et al. 1990, Balcomb and Jones 1983). These insights can be readily used for parametric analysis and design optimization. See Section "Discussion" for more information.

METHODOLOGY

The concept of the methodology is rather simple – based on the profile of the room temperature and corresponding required thermal output from the active BITES system, the profile of required thermal energy injection to the active BITES system will be

obtained using frequency domain transfer functions. In this section, the main theories and techniques will be discussed and exemplified. Detailed approaches and calculations will be presented in the next section. Sometimes, "BITES" will be used to represent "active BITES systems" for short.

Modeling Active BITES Systems

One-dimensional thermal model for active BITES systems is used in this study. Studies have showed that one dimensional (normal to the room-side surface of the slab) thermal model can approximate the thermal behavior of these systems well under conditions of practical interest (Barton et al. 2002, Chen et al. 2010b, Ren and Wright 1998, Strand 1995). Figure 2 shows a portion of the cross section of the active BITES floor system adopted for demonstration in this study. The original cross section is transformed into an equivalent cross section by replacing the original core conditioning system (e.g. air channels or water pipes) with an imaginary thickness-less "source" layer. The transformed cross section has the same area as the original. Heat flux is from conditioning fluids such as air or water. This transformation allows the heat transfer to be treated as one dimensional normal to the room-side surface of the floor. Chen et al. (2013) presented the calculation of core-conditioning heat flux from fluids.
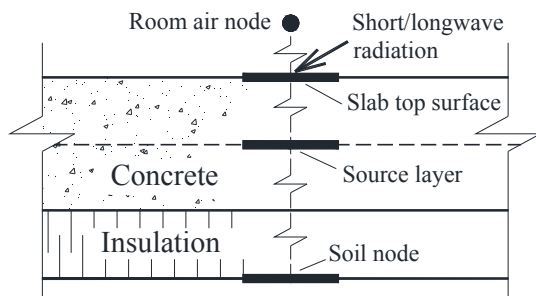

Figure 2. Thermal network of an active BITES floor with its cross section transformed

The cross sections can represent either a slab on-grade or an intermediate floor. The insulation is optional for intermediate floors. It will be used if building designers would like to orientate the heat to only one side of the slab. The insulation layer can

also represent the false ceiling and the air cavity in the ceiling, from the view point of heat transfer.

Source Layer Temperature and Thermal Energy Injection

Using discrete frequency response modeling for an assembly consisting of N layers of material (Figure 3), the oscillatory responses of heat flux ${}_{0}^{1}\tilde{p}_{i,h}$ and temperature ${}_{0}^{1}\tilde{T}_{i,h}$ at surface 0 of layer 1 due to excitations ${}_{l}^{N}\tilde{p}_{i,h}$ and ${}_{l}^{N}\tilde{T}_{i,h}$ on surface l of layer N can be calculated with Eq. (1) (Carslaw and Jaeger 1959, Kimura 1977). The right-hand side subscript i means the ith time interval, and h is the harmonic index. The mean responses can be obtained in a similar way with the transfer functions matrix ${}_{trs}^{1\leftarrow N}[M]_h$ replaced with a thermal resistance matrix. Then the total responses in frequency domain at surface 0 will be ${}_{0}^{1}\hat{T}_i = {}_{0}^{1}\bar{T} + \sum_{h=1}^{H}\left({}_{0}^{1}\tilde{T}_{i,h}\right)$, and ${}_{0}^{1}\hat{p}_i = {}_{0}^{1}\bar{p} + \sum_{h=1}^{H}\left({}_{0}^{1}\tilde{p}_{i,h}\right)$. Time domain values can then be obtained through ${}_{0}^{1}T_i = Re\left\{{}_{0}^{1}\hat{T}_i\right\}$ and ${}_{0}^{1}p_i = Re\left\{{}_{0}^{1}\hat{p}_i\right\}$, where $Re\{\ \}$ takes the real part value from the complex number. See appendix for more information on discrete frequency response modeling.

$$\begin{bmatrix} {}_{0}^{1}\tilde{T}_{i,h} \\ {}_{0}^{1}\tilde{p}_{i,h} \end{bmatrix} = {}_{trs}^{1\leftarrow N}[M]_h \cdot \begin{bmatrix} {}_{l}^{N}\tilde{T}_{i,h} \\ {}_{l}^{N}\tilde{p}_{i,h} \end{bmatrix} \tag{1}$$
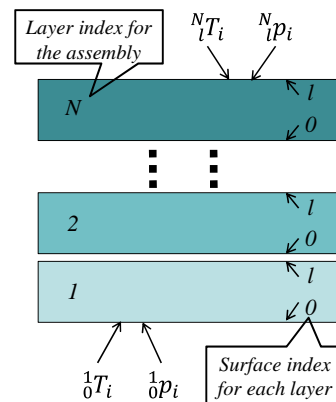

Figure 3. Schematic of an assembly consisting of N layers, and its excitations

Similarly, let room air node be at surface l of N layer, and excitations ${}_{rm}\tilde{T}_i$ and ${}_{CR.B}\tilde{p}_i$ be the room air temperature and the heat flux from the BITES exposed surface to the room air, respectively. Also, let BITES source layer (Figure 2) be at surface 0 of layer 1, and surface 0 be adiabatic to its exterior

boundary (e.g. the concrete underneath the source layer). The responses $_{sc}\tilde{T}_i$ and $_{sc}\tilde{p}_i$ at time interval i at source layer can be calculated with Eq. (2), given that $_{rm}\tilde{T}_i$ and $_{CR.B}\tilde{p}_i$ are known. In reality, source layer (i.e. surface 0 of layer 1) is not adiabatic to the exterior boundary of the assembly. Heat flux through BITES to the room air node will also include those from the heat sources and temperatures of the exterior boundary. A portion of source heat flux will also be distributed to the exterior boundary. Detailed calculations will be presented later.

$$\begin{bmatrix} _{sc}\tilde{T}_{i,h} \\ _{sc}\tilde{p}_{i,h} \end{bmatrix} = {}^{sc \leftarrow rm}_{trs}[M]_h \begin{bmatrix} _{rm}\tilde{T}_{i,h} \\ _{CR.B}\tilde{p}_{i,h} \end{bmatrix} \qquad (2)$$

Looking at the energy balance at the room air node, $_{CR.B}p$ is the combined convective and radiative thermal outputs to the room from the room-side exposed surface of the BITES. It compensates the room air heat gain/loss, and hence maintains $_{rm}T$ at its set values.

In the frequency domain modeling used in this study, discrete complex variables and transfer functions are used. Time-series values (e.g. temperature readings in different time intervals) are represented with complex discrete Fourier series (DFS). See appendix for more information. Furthermore, the thermal characteristics of all material are assumed to be linear and time-invariant (e.g. conductivity and specific heat capacity do not depend on temperature or time).

Room Air Temperature Profile

In the methodology developed in this study, the room temperature is used to leverage the operation of the active BITES systems. In addition to the consideration that the thermal behavior of the room and its BITES are strongly coupled, another main reason for adopting this approach is that appropriate room temperature is critical both to thermal comfort requirement and to improve the overall thermal and energy performance of the building.

In this study, room air temperature is set as a function of the exterior temperature, solar radiation, and the time constant of the room. This temperature setting approach enhances the room energy performance to a certain extent. Further optimization of temperature profile can be adopted, such as taking internal heat gain into consideration, and weighting factors accounting peak hours and utility fee structure. Approaches for the optimization of room temperature profile are worth studying in the future.

A room air temperature profile during a space heating period (Figure 4) is used here for brief demonstration. Two-day periods are used in this study mainly for evaluating the thermal and energy performance of the BITES operations in relatively long periods. At first, a bounding room temperature envelope is constructed using 22.5°C as the set point with a throttling range of 5°C centered at the set point. In other words, the room temperature will not be lower than 20°C or higher than 25°C. These two values can and should be able to be adjusted by occupants. In general, the temperature difference between the room and the exterior solar-air temperature (ASHRAE 2009d) will be minimized within the allowable room temperature range, in order to reduce space conditioning load. High solar-air temperature will result in a high room air temperature, and low room air temperature for low solar-air temperature. Solar-air temperature equals to exterior temperature after sunset. The room temperature follows the solar-air temperature with a first-order time lag (ASHRAE 2009b). For example, the start of the rise of the room temperature (hour 9.5) lags behind the rise of the solar-air temperature (hour 7.5). The time lag is calculated using a function of the time constant of the effective thermal capacitance of the room air. When solar-air temperature is ideal for building pre-heating/-cooling, the room air temperature will change faster; otherwise, the room temperature will response naturally.
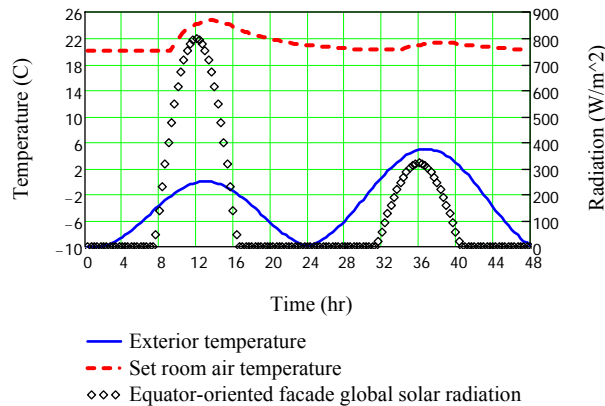
Figure 4. Weather conditions and room air temperature set profile during a two-day space heating period

The room air temperature profile obtained in the above approach approximates the natural response of the room to its boundary condition variation, and avoids sudden changes on the thermal output requirement of the active BITES systems. As shown in Figure 4, the room air temperature rises during sunny period to allow solar heat gain stored in the BITES and the rest of the room. The profile also reduces the space heating load after sunset by reducing the temperature difference between exterior and interior. With respect to thermal comfort, this temperature profile complies with upper and lower temperature limits and avoids rapid changes. As shown later in Figure 9, this approach also allows off-peak pre-heating, and enables use of solar thermal energy for heating during the daytime, for both room and its BITES.

Space Conditioning Load Profile

After setting the room air temperature profile, another measure is needed to estimate the space conditioning loads (i.e. the required thermal output from the BITES system). In this study, an explicit finite difference thermal model of the room is created to perform this estimation. Besides the forward approaches (or physical thermal models) such as the one used in this study, data-driven (inverse) models, such as Black-Box (empirical) or Gray-Box types of models (ASHRAE 2009a), can also be used to estimate the space conditioning load (Armstrong et al. 2006a, b, ASHRAE 2009a, Braun et al. 2001). Data-driven models can be trained and further fine-tuned

with filed-measured (i.e. online) data (Nassif et al. 2008). Self-tuning models may be more appropriate because of the various uncertainties of the built environment and occupant behavior. Selecting suitable approach for space conditioning load estimation is beyond the scope of this study.

The space conditioning load estimation in this study uses a finite difference model. This finite difference thermal model is also used to help with the development and validation of the control methodology, as shown later. A 10.5m (length) x 3m x 3m room is used for demonstration. This room has five square meters of windows on the long façade facing the equator. An active BITES system (Figure 2) is located on the floor of the room. Table 1 lists the key parameters of the room. The finite difference thermal model of the room will calculate the room's space conditioning loads based on the room air temperature set profiles.

Table 1: Key parameters of the room thermal model

Parameters	Values	Note
Concrete slab thickness	0.3 meters	
Location of source layer in concrete	0.108 meters below the top concrete surface	Source layer in Figure 2
Thermal insulation under concrete slab	0.5 W/m²/K	
Total envelope thermal conductance	32 W/K	Ventilation and infiltration heat/gain is included
Room air temperature	Set point of 22.5°C, and throttling range of 5°C	
Effective thermal capacitance of indoor objects	50 times room air capacitance	Includes the thermal mass of wallboards (e.g. gypsum wallboard) and furniture
Thermo-	840 J/kg/K for	Constant

physical properties of concrete	specific heat; 2200 kg/m³ for density; 1.7 W/m/K for conductivity	
Thermo-physical properties of air	1300 J/m³/K for volumetric heat capacity	Constant
Soil node temperature	10°C	Constant

The set profile of room air temperature for a winter period and the weather conditions are shown in Figure 4. The required space conditioning (i.e. thermal output required from the active BITES system) is calculated with the room thermal model and shown in Figure 5. The room air heat gain/loss is due to internal heat gain (e.g. appliance, human body), transmitted solar radiation, ventilation, infiltration, and conduction through envelope. The small spikes are due to cooking. Some key treatments in the calculation are as follows:
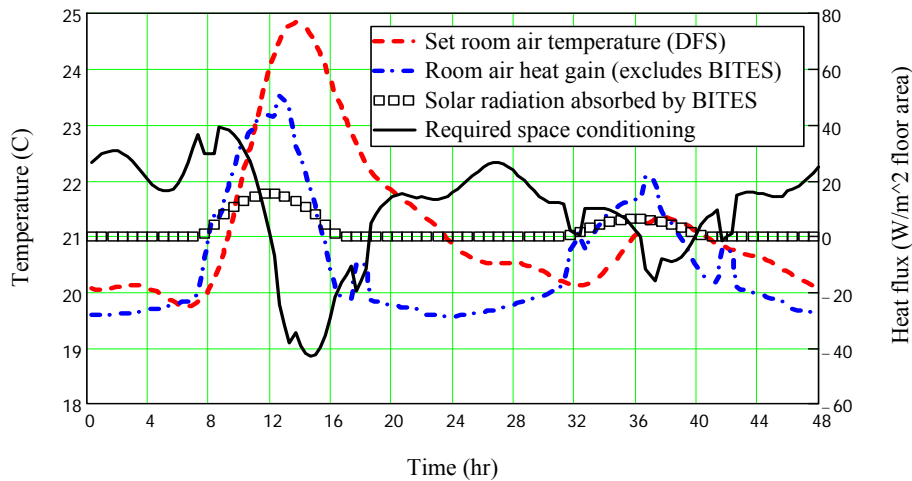

Figure 5. DFS represented room air temperature profile and corresponding energy profiles (negative value in heat gain means heat loss; negative value in space conditioning means space cooling is required)
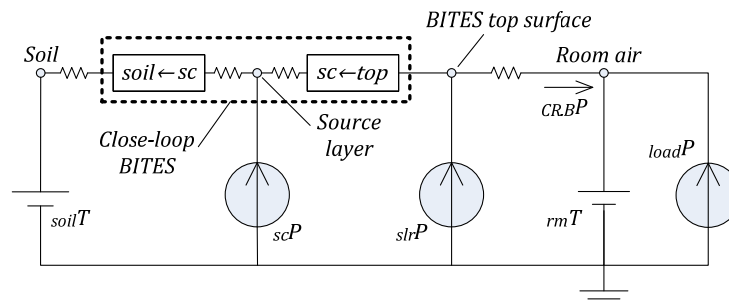

Figure 6. Simplified thermal network of room with a close-loop BITES system sitting on soil (Figure 2)

- The room air temperature set profile is represented with complex DFS (Figure 5, 6 harmonics is used for DFS). Then, the DFS-represented values will be converted back to time domain and used to calculate the space conditioning loads;
- When calculating the space conditioning load, the active BITES floor including the solar radiation impinging on it is assumed to be adiabatic to the rest of the room;
- The required thermal output of the BITES including the release of its absorbed solar radiation is set equal to the room space conditioning load.

APPLICATION

In this section, control methodology and detailed calculation approach will be demonstrated on a close-loop BITES floor system (Figure 1) in the room described previously. The profiles of the room air temperature and the required thermal output are shown in Figure 5. The thermal model of the active BITES floor is shown in Figure 2. The calculated thermal injection will be validated with the explicit finite difference model described above. During validation, the room air temperature is not set, but calculated based on the thermal energy injection to the active BITES floor and thermal energy balance of the room. Results for space heating scenario and further treatment for thermal energy injection are presented below in details. Results for cooling scenario are presented briefly after. In the following paragraphs and figures, "predicted" values are calculated using the methodology, while "simulated" values are from the validations.

Figure 6 shows the thermal network of the close-loop BITES floor with its boundary conditions. In addition to the convective and radiative heat exchange with the room, the exposed surface of BITES receives solar radiation $_{slr}p$ transmitted through the windows.

Formulation

The convective heat transfer coefficient (CHTC) between the BITES exposed surface and the room air (i.e. air film in Figure 2) is highly temperature-potential dependent – the heat transfer between these two nodes is not linear). Without proper treatment, the air film cannot be included in the linearity-assumed assembly. Otherwise, significant errors will be caused. Considering the fact that instant thermal output from the exposed surface equals to the required thermal input $_{CR.B}p$ to the room air node (i.e. no thermal capacitance between these two nodes), the thermal output from the exposed surface and the surface temperature $_{top}T$ are used to calculate the source layer temperature $_{sc}T$ and its thermal energy injection requirement $_{sc}p$ in this study. In this way, the air film is not included in the assembly. When the room air temperature $_{rm}T$ and the required thermal output from the top surface $_{CR.B}p$ are known, $_{top}T$

can be obtained by solving Eq. (3) and (4) simultaneously or by iterations.

$$_{top}T_i = {_{CR.B}p_i}/{_{top}h_i} + {_{rm}T_i} \tag{3}$$

$$_{top}h_i = {_{c.top}h_i} + {_{r.top}h}$$
$$= fn\left({_{rm}T_i}, {_{top}T_i}\right) + {_{r.top}h_i} \tag{4}$$

where $fn(a, b)$ means a function of a and b. $_{top}h$ is a combined convective and radiative heat transfer coefficient. An empirical equation Eq. (5) (ASHRAE 2009c) is used in this study to determine the convective part $_{c.top}h$. Constant value of 4.5 W/m²/K can be used for the radiative part $_{r.top}h$ under practical conditions (i.e. temperature difference between floor surface and the rest of room is less than 10°C) with negligible errors.

$$_{c.top}h = 2.42 \cdot \frac{|\Delta T|^{0.31}}{_{rm.c}L^{0.08}}$$

when heating upward or cooling download, or

$$_{c.top}h = 0.2 \cdot \frac{|\Delta T|^{0.25}}{_{rm.c}L^{0.25}} \tag{5}$$

when heating downward or cooling upward

where ΔT is the temperature difference between the surface ($_{top}T$ in this case) and the room air. $_{rm.c}L$ is the characteristic length of the room.

The combined convective and radiative thermal output $_{CR.B}p$ is a combined output from different sources (e.g. temperature potentials and heat flux) (Eq. (6)). Since the thermal system in question is linear, different portions of $_{CR.B}p$ can be calculated separately. Then the required thermal energy injection $_{sc}p$ equals to the difference between the known $_{CR.B}p$ and outputs from other sources. The following equations calculate the oscillatory responses of the variables in question. The mean responses and then the final values in time domain are calculated in similar ways as discussed in Subsection 0. Subscript h for harmonic is omitted.

$$_{CR.B}\tilde{p}_i = {}_{sc\_top}\tilde{p}_i + {}_{slr}\tilde{p}_i + {}_{soil\_top}\tilde{p}_i \qquad (6)$$

where $_{slr}p$ is the transmitted solar radiation absorbed by the BITES top surface

The oscillatory part of heat flux $_{soil\_top}\tilde{p}$ flowing to the floor top surface due to temperature difference between top surface and soil can be calculated with Eq. (7).

$$_{soil\_top}\tilde{p}_i = {}_{soil}\tilde{T}_i \cdot {}^{soil\leftarrow top}a21 + {}_{top}\tilde{T}_i \cdot {}^{soil\leftarrow top}a22 \qquad (7)$$

where $a22$ and $a21$ are from admittance matrix $_{adm}[M]$ of assembly $soil \leftarrow top$ (i.e. the concrete and the insulation layers in Figure 2). See appendix for more detail on admittance matrix.

The remaining portion of $_{CR.B}p$ due to thermal energy injection at source layer can be calculated according to Eq. (8):

$$_{sc\_top}\tilde{p}_i = {}_{CR.B}\tilde{p}_i - {}_{slr}\tilde{p}_i - {}_{soil\_top}\tilde{p}_i \qquad (8)$$

Hence, the required thermal energy injection can be obtained by reversing heat flow division

$$_{sc}\tilde{p}_i = {}_{sc\_top}\tilde{p}_i \cdot \frac{^{soil\leftarrow top}t12}{^{soil\leftarrow sc}t12} \qquad (9)$$

where $t22$ and $t21$ are from two different transmission matrices $_{trs}[M]$. See appendix for more information on transmission matrices.

The mean response of the heat flow $_{sc}\bar{p}$ can be calculated similarly.

$$_{soil\_top}\bar{p} = \left(_{soil}\bar{T} - {}_{top}\bar{T}\right)/^{soil\leftarrow top}r$$

and $\quad _{sc}\bar{p} = {}_{sc\_top}\bar{p} \cdot \frac{^{soil\leftarrow top}r}{^{soil\leftarrow sc}r}$

where $^{soil\leftarrow top}r$ is the thermal resistance between soil and top surface, and $^{soil\leftarrow sc}r$ is the thermal resistance between soil and source layer.

Finally, the required thermal energy injection at source level (or layer) in time domain

$$_{sc}p_i = {}_{sc}\bar{p} + Re\left\{\sum_{h=1}^{H} {}_{sc}\tilde{p}_{i,h}\right\} \qquad (10)$$

After obtaining the required $_{sc}p$, the source layer temperature $_{sc}T$ is also required in order to calculate the required inlet temperature of the fluids. Even though Eq. (2) is not directly shown in the above equations, these equations are derived based on Eq. (2) and the theory behind it.

Preliminary Results for Space Heating Scenario
The thermal energy injection at source layer predicted using Eq. (7) to (10) is used in the finite difference thermal model to simulate the thermal performance of the room. Figure 7 and Figure 8 show the thermal performance of the room and its active BITES floor. Both the temperatures of the room air and the floor top surface (Figure 8) comply with thermal comfort requirement. As seen in Figure 7, even though the thermal output does not precisely follow the required space conditioning, the resulted room air temperature closely matches the set profile well. This is due to the high thermal mass characteristic of the room and the BITES. Using more harmonics for DFS representation will improve the matching; however, this is not necessary as the room temperature setting is well satisfied.
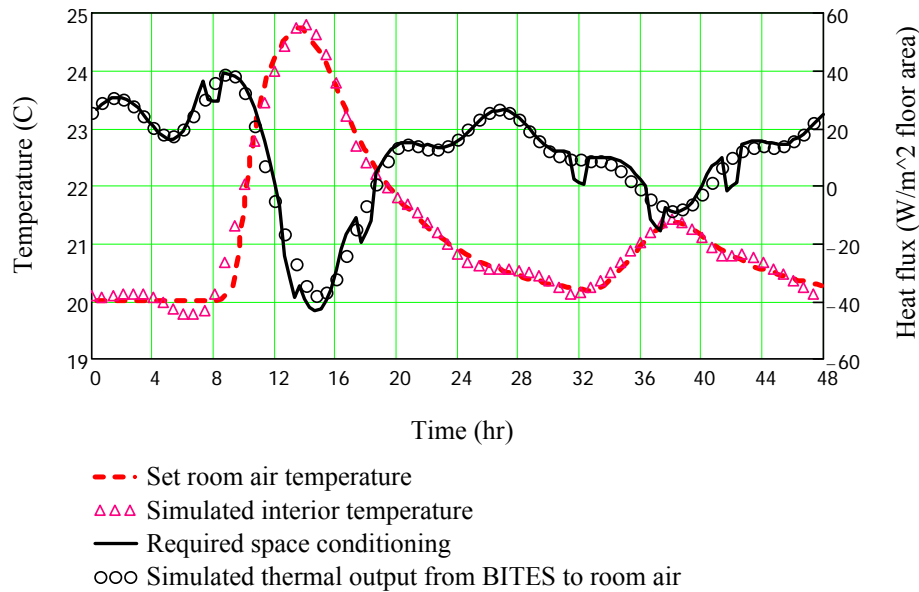
Figure 7. Comparison of set and simulated room air temperatures and BITES thermal outputs
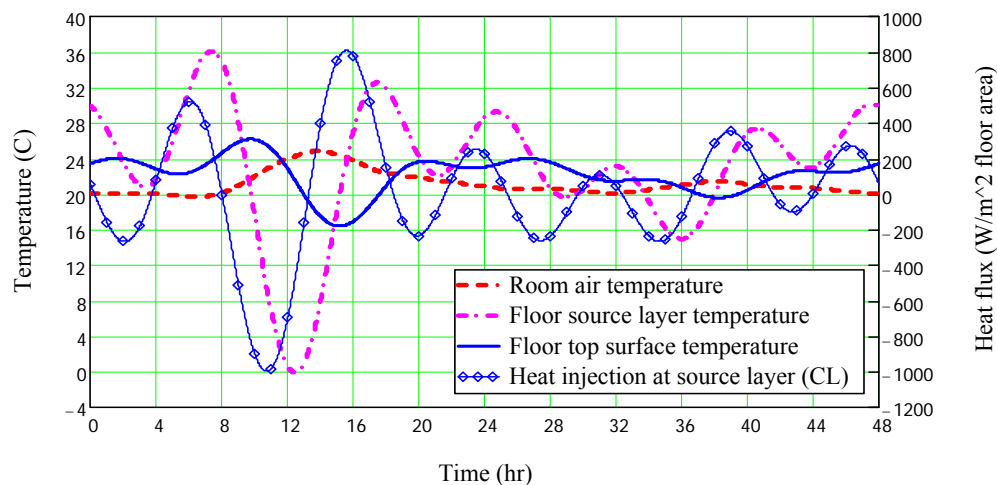

Figure 8. Simulated thermal performance based on predicted thermal energy injection

Treatment on Thermal Energy Injection

Looking at Figure 8, thermal energy injection switches frequently between heating and cooling with large magnitudes. This is due to the precise control of the room air temperature; however, from the energy point of view, this is not desirable. Thermal energy is wasted in counteracting itself, and the cycling of mechanical systems supplying thermal energy is too frequent.

This fluctuation problem can be avoided by taking the advantage of the high thermal mass characteristic of the active BITES system, and using the principle of energy conservation law. Without

changing the net amount of energy injection (summation of numerical values, positive for heating) within a certain period, the dynamic BITES temperature will not change significantly from the original. Hence, the original energy injection profile can be smoothed in a way that later injection does not counteract the previous one. A preliminary formulation is provided here for the smoothing treatment – the original energy injection is averaged with that of adjacent time intervals and then replaced by the average value (Eq. (11)).

$$_{sc}p_i = \frac{_{sc}p_{i-1} + {}_{sc}p_i + {}_{sc}p_{i+1}}{3} \qquad (11)$$

Under certain weather conditions, BITES thermal output is necessary to switch between cooling and heating to keep room air at desired temperature. Hence, the goal for the smoothing treatment in this study is to avoid switching between cooling and heating more than once (double switching) within the period of the first 24 hours. A search action will be performed. Once double switching is detected within this 24-hour period, thermal energy injection at all time intervals within the whole modeling period (48 hours in this study) will be smoothed using Eq. (11). This averaging will

be performed until double switching is eliminated within the search horizon (i.e. first 24 hours).

Figure 9 shows the room thermal behavior and energy performance after smoothing the thermal energy injection using Eq. (11). The resulted room temperature profile generally follows the set profile, being slightly lower than the set values during the first day. Even though the resulted room temperature profile does not match the set profile, but it serves the same purpose – active BITES system is properly controlled and thermal comfort is provided. If desired, this imperfection can be resolved by adjusting the heating set point or applying a scaling factor to thermal energy injection. Scaling factor 1.2 is suitable for this case.
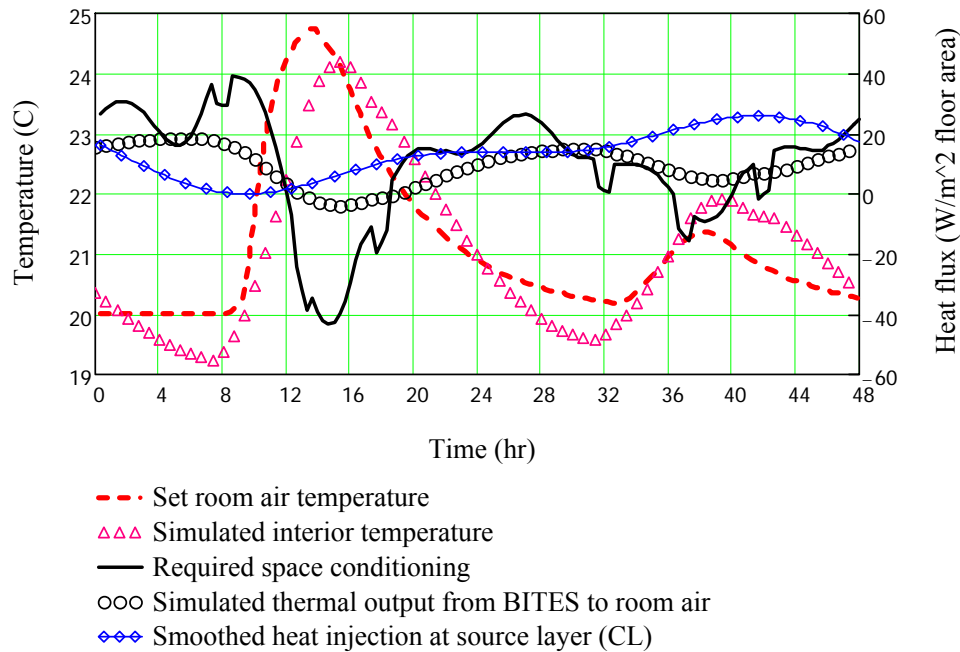

Figure 9. Comparison of set and simulated room air temperatures and BITES thermal output after smoothing thermal energy injection

DISCUSSION

By comparing the peaks and lows in Figure 7 and Figure 8, there is a time lag of about four hours between input (i.e. thermal energy injection at source layer) and the output of the active BITES system (e.g. hour 11 and hour 15 in Figure 8). The time lag between the output of the BITES system and the response of the room is about 5.5 hours (e.g. hour 8.5 and hour 14 in Figure 7 or Figure 8). Hence, the time

lag between the input of the BITES system and the response of the room is about nine to ten hours. These significant time lags are critical design factors to be considered. This need reveals the important application of frequency domain functions in design optimization.

With frequency domain transfer functions, the systems' time lags can be readily seen from the phase angles (or arguments) of the corresponding transfer

functions. For example, the time lag between the input and output of the close-loop BITES system used in the above study is related to the phase angle of the transfer functions used for heat flow division (e.g. Eq. (9)). By looking at Figure 9, the principal frequency of the thermal energy injection is one cycle (i.e. 2π) per 24 hours (i.e. one harmonic). Since the phase angle from one harmonic is

$$Arg\left\{\frac{\left[{}^{soil\leftarrow sc}t12\right]_{h=1}}{\left[{}^{soil\leftarrow top}t12\right]_{h=1}}\right\} = -1.043\ radian$$

where $Arg\{\ \}$ calculates the argument or phase angle of a complex number

The time lag approximately equals to $-1.043\ radian \cdot (24\ hr/2\pi) = -3.985\ hr$. This value precisely reflects the value from observing the actual thermal response of the room (i.e. Figure 7 and Figure 8). In similar ways, time lags and magnitudes of other important variables can be obtained by analyzing the properties of corresponding frequency domain transfer functions (Athienitis 1994). Hence the overall design optimization can be achieved on such relative bases.

CONCLUSIONS

In this study, a methodology for predictive control of active building-integrated thermal energy storage (BITES) systems using frequency domain modeling is presented. The main idea of this methodology is to use frequency domain transfer functions to predict the required thermal energy injection based on the desired room air temperature and the corresponding space conditioning load. The objective of the methodology is to satisfy the thermal comfort requirement for room temperature, as well as to enhance the building energy performance.

The application of this methodology on a close-loop active BITES system is presented. The formulations, relevant treatments, and results are presented. The methodology is proven capable of predicting the required thermal energy injection. General procedure is summarized as follows:

(1) Collect weather forecast information (solar radiation and exterior temperature);

(2) Set the future room air temperature profile with respects to thermal comfort and energy saving, and then precede it with historic room air temperature. Represent the merge profile with complex discrete Fourier series (DFS);

(3) Estimate the required future thermal output of active BITES systems based on the DFS represented future room air temperature, and then precede it with historic thermal output. Represent the merged profile with complex DFS;

(4) Use the DFS-represented room air temperature and thermal output to calculate the required thermal energy injection to the active BITES system;

(5) Apply smoothing treatment to the calculated thermal energy injection;

With the demonstration, the typical thermal behavior and energy performance of active BITES systems under practical operations are also shown.

NOMENCLATURES

Symbols

$\wedge$	DFS or complex frequency form
$-$	(Overhead bar) mean value/response
$\_$	(Underscore) a_b means from a to b
$\sim$	Oscillatory response
$\leftarrow$	Order of layers in an assembly. $1 \leftarrow N$ means the assembly contains layers from 1 to N, and the excitations are on surface l of layer N
[ ]	Matrix or vector

Greek

ρc	Volumetric heat capacity (J/m³/K)

English

a	Admittance matrix element or a numerical value or
A	Advective/advection or a numerical value
$Area$	Surface area
$Arg\{\ \}$	Argument (phase angle) of the complex number
B	BITES
c	Coefficients, combined, or convective
C	Thermal capacitance (J/K)

CR	Combined convection and radiation
i	Index of time step
k	Thermal conductivity (W/m/K)
h	Convective heat transfer coefficient or harmonic index
H	Total number of harmonics used in the modeling
M	Matrix of transfer functions
p	Heat flux or power per unit area (W/m^2)
r	Thermal resistance per square meter (m^2·K/W)
rm	Room or room air
$Re\{\ \}$	Real part of the complex number
sc	Source layer
trs	Transmission matrix
t	Time (seconds) or transmission matrix element
T	Temperature (°C)

Acronyms

ACH	Air change per hour. Air flow rate in terms of how many times of room volume in one hour
BITES	Building-integrated thermal energy storage
CHTC	Convective heat transfer coefficient
CL	Close-loop BITES systems
DFS	Discrete Fourier series
TES	Thermal energy storage

Key Variables

$^{soil \leftarrow top}a21$	The element at the second row and first column of the admittance matrix $^{soil \leftarrow top}_{adm}[M]$ of the assembly between soil and top floor surface
$_{top}h$	Combined heat transfer coefficient on BITES top surface
$^{1 \leftarrow N}_{adm}[M]_h$	Admittance matrix of the hth harmonic for an assembly composed of layers 1 to N
$_{CR.B}p$	Combined convective and radiative thermal output of BITES system
$_{load}p$	Space conditioning load or required thermal output from the BITES systems
$_{sc}p$	Source thermal energy injection
$_{slr}p$	Transmitted solar radiation absorbed by BITES top surface

$_{soil\_top}p$	Heat flux following to the floor top surface due to temperature difference between top surface and soil
$^{soil \leftarrow top}r$	Thermal resistance between soil and floor top surface
$^{1 \leftarrow N}_{trs}[M]_h$	Transmission matrix of the hth harmonic for an assembly composed of layers 1 to N
$_{rm}T$	Room air temperature
$_{sc}T$	Floor source layer temperature
$_{soil}T$	Soil temperature
$_{top}T$	BITES top surface temperature

REFERENCES

Armstrong, P. R., S. B. Leeb and L. K. Norford. 2006a. Control with building mass - Part I: Thermal response model. *ASHRAE Transactions,* 112(1): 449-461.

Armstrong, P. R., S. B. Leeb and L. K. Norford. 2006b. Control with building mass - Part II: Simulation. ASHRAE Transactions, 112(1): 462-473.

ASHRAE. 2007. Thermal Storage. ASHRAE Handbook - HVAC Applications. SI ed. Atlanta, GA, US: American Society of Heating Refrigerating and Air-Conditioning Engineers (ASHRAE).

ASHRAE. 2009a. Energy estimating and modeling methods. ASHRAE Handbook - Fundamentals. SI ed. Atlanta, GA, USA: American Society of Heating, Refrigerating, and Air-Conditioning Engineers (ASHRAE).

ASHRAE. 2009b. Fundamentals of Control. ASHRAE Handbook - Fundamentals. SI ed. Atlanta, GA, USA: American Society of Heating, Refrigerating, and Air-Conditioning Engineers (ASHRAE).

ASHRAE. 2009c. Heat transfer. *ASHRAE Handbook - Fundamentals.* SI ed. Atlanta, GA, USA: American Society of Heating, Refrigerating, and Air-Conditioning Engineers (ASHRAE).

ASHRAE. 2009d. Non-residential cooling and heating load calculations. *ASHRAE Handbook - Fundamentals.* SI ed. Atlanta, GA, USA: American Society of Heating, Refrigerating, and Air-Conditioning Engineers (ASHRAE).

Athienitis, A. K. 1994. *Building Thermal Analysis,* Boston, MA, USA, MathSoft Inc.

Athienitis, A. K., M. Stylianou and J. Shou. 1990. A methodology for building thermal dynamics studies and control applications. *ASHRAE Transactions,* 96(2): 839-848.

Athienitis, A. K., H. F. Sullivan and K. G. T. Hollands. 1987. Discrete Fourier-Series Models for Building Auxiliary Energy Loads Based on Network Formulation Techniques. *Solar Energy,* 39(3): 203-210.

Balcomb, J. D. and R. W. Jones. 1983. Passive solar design analysis. *In:* Los Alamos National Laboratory, ed. *Passive Solar Design Handbook.* Boulder, US: American Solar Energy Society.

Barton, P., C. B. Beggs and P. A. Sleigh. 2002. A theoretical study of the thermal performance of the TermoDeck hollow core slab system. *Applied* Thermal *Engineering,* 22(13): 1485-1499.

Bird, J. O. 2007. *Electrical circuit theory and technology,* Boston, US, Newnes.

Braun, J. E. 2003. Load control using building thermal mass. Journal *of Solar Energy Engineering-Transactions of the ASME,* 125(3): 292-301.

Braun, J. E., K. W. Montgomery and N. Chaturvedi. 2001. Evaluating the performance of building thermal mass control strategies. *HVAC&R Research,* 7(4): 403-428.

Carslaw, H. S. and J. C. Jaeger. 1959. *Conduction of heat in solids,* Oxford,, Clarendon Press.

Chen, W.-K. 1983. *Linear networks and systems,* Monterey, Ca, US, Brooks/Cole Engineering Division.

Chen, Y., A. Athienitis and K. Galal. 2013. Frequency domain and finite difference modeling of ventilated concrete slabs and comparison with field measurements: Part 1, modeling methodology. *International Journal of Heat and Mass Transfer,* in press.

Chen, Y., A. K. Athienitis and K. Galal. 2010a. Modeling, design and thermal performance of a BIPV/T system thermally coupled with a ventilated concrete slab in a low energy solar house: Part 1, BIPV/T system and house energy concept. *Solar Energy,* 84(11): 1892-1907.

Chen, Y., K. Galal and A. K. Athienitis. 2010b. Modeling, design and thermal performance of a BIPV/T system thermally coupled with a ventilated concrete slab in a low energy solar house: Part 2, ventilated concrete slab. *Solar Energy,* 84(11): 1908-1919.

Hadorn, J.-C. (ed.) 2005. *Thermal Energy Storage for Solar and Low Energy Buildings*: International Energy Agency (IEA) Solar Heating and Cooling Task 32 - Advanced storage concepts for solar and low energy buildings, IEA.

Kimura, K.-I. 1977. Unsteady state heat conduction through walls and slabs. *In:* K.-I. Kimura, ed. *Scientific basis for air-conditioning.* London, UK: Applied Science Publishers Ltd.

Kreyszig, E. 2006. *Advanced engineering mathematics,* Hoboken, NJ, John Wiley.

Nassif, N., S. Moujaes and M. Zaheeruddin. 2008. Self-tuning dynamic models of HVAC system components. *Energy and Buildings,* 40(9): 1709-1720.

Pipes, L. A. 1957. Matrix analysis of heat transfer problems. Journal *of the Franklin Institute,* 263(3): 195-206.

Ren, M. J. and J. A. Wright. 1998. A ventilated slab thermal storage system model. *Building and Environment,* 33(1): 43-52.

Strand, R. K. 1995. *Heat source transfer functions and their* application *to low temperature radiant heating systems.* Ph.D. 9543736, University of Illinois at Urbana-Champaign.

APPENDIX

A.   Quick Review of Frequency Domain Modeling

Discrete Fourier series (DFS) representation of excitations

Given a time series of discrete values, in Eq. (A-1),

$$[A]_\mathrm{I} = [A_1, A_2, A_3 \ ... \ A_i \ ... \ A_I] \qquad (A\text{-}1)$$

where $i = 1, 2 \ ... I$, is the time-series index, indicating the time (i.e. $t = \Delta t \cdot i$) at which the value is sampled. Δt is the time interval of data sampling. I indicates how many values are given.

Its complex DFS representation can be approximated using Eq. (A-2). See Chen (1983) and Kreyszig (2006) for more details on Fourier series and discrete Fourier series.

$$\hat{A}_i \cong a_0 + 2 \sum_{h=1}^{H} \left(a_h \cdot e^{jh\omega_f i \Delta t} \right)$$

$$= a_0 + 2 \cdot \sum_{h=1}^{H} \left(a_h \cdot e^{jh\frac{2\pi}{T}i} \right)$$

(A-2)

where accent "∧" means DFS or complex frequency form, and $\omega_f = 2\pi/P$ is the fundamental angular frequency. P is the analysis period in seconds ($P = \Delta t \cdot I$). H is a positive integer indicating the number of harmonics are used in the approximation.

$$a_0 = \frac{1}{I} \sum_{i=1}^{I} \left(A_i \cdot e^{-j0\frac{2\pi}{T}i} \right) = \frac{1}{I} \sum_{i=1}^{I} A_i$$

$$a_h \cong \frac{1}{I} \sum_{i=1}^{I} \left(A_i \cdot e^{-jh\omega_f i \Delta t} \right) = \frac{1}{I} \sum_{i=1}^{I} \left(A_i \cdot e^{-jh\frac{2\pi}{T}i} \right)$$

$$A_i \cong Re\{\hat{A}_i\}$$

Frequency domain modeling

See references (Athienitis et al. 1987, Carslaw and Jaeger 1959, Chen et al. 2013, Kimura 1977, Pipes 1957) for the application of DFS in frequency domain modeling. The overall transmission matrix for a N-layer assembly simply equals to the product of the individual transmission matrix in the order corresponding to their locations in the assembly (Eq. (A-3)).

$$^{1\leftarrow N}_{trs}[M]_h = {}^{1}_{trs}[M]_h \cdot {}^{2}_{trs}[M]_h \\ \cdot {}^{3}_{trs}[M]_h \ \cdots \ \cdot {}^{N}_{trs}[M]_h$$

(A-3)

where left-hand-side superscript "$1 \leftarrow N$" indicates this transmission matrix is of the assembly containing layers from 1 to N. As indicated by Eq. (A-3), the temperature and heat flux on surface l of layer N have to be the excitations for this formulation $^{n}_{trs}[M]_h$ is the transmission matrix of layer n (Eq. (A-4)). In this study, surfaces 0 and l are the opposite outer surfaces of any layer, such as the room air and the wall surface in an air film layer. It is important to

note that the values in the excitation vectors are of various harmonics h, as in their DFS representations.

$$^{n}_{trs}[M]_h$$
$$= \begin{bmatrix} cosh(^{n}l \cdot \gamma_h) & \dfrac{sinh(^{n}l \cdot \gamma_h)}{^{n}k \cdot \gamma_h} \\ ^{n}k \cdot \gamma_h \, sinh(^{n}l \cdot \gamma_h) & cosh(^{n}l \cdot \gamma_h) \end{bmatrix}$$

(A-4)

where ^{n}l is the thickness of layer n, and ^{n}k is the thermal conductivity (W/m/K). $\gamma_h = \sqrt{j\omega_f h / {}^{n}\alpha}$, and $^{n}\alpha = {}^{n}k / {}^{n}\rho \cdot {}^{n}c$ is the thermal diffusivity of the material (m²/sec) of layer n.

For a layer that can be considered as purely resistive/conductive (e.g. insulation, air film), the transmission matrix becomes $_{trs}[M]_h = \begin{bmatrix} 1 & r \\ 0 & 1 \end{bmatrix}$. r is the thermal resistance of the corresponding layer. For an exterior air film, $r = 1/{}_{cnv}h$, with $_{cnv}h$ being the exterior CHTC.

Let $\quad _{trs}[M]_h = \begin{bmatrix} t11_h & t12_h \\ t21_h & t22_h \end{bmatrix}$

and $\quad _{adm}[M]_h = \begin{bmatrix} a11_h & a12_h \\ a21_h & a22_h \end{bmatrix}$

then the admittance matrix can be calculated as

$a11_h = t22_h/t12_h$; $a12_h = -1/t12_h$; $a21_h = 1/t12_h$; $a22_h = -t11_h/t12_h$.
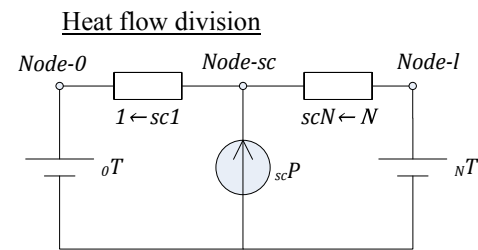
Heat flow division

Figure 10: Thermal network (node 0 is the outermost node of assembly $1 \leftarrow sc1$, while node l is the outermost node of assembly $scN \leftarrow N$. Source node sc is in-between the two assemblies)

For the heat sources that are not located at the two outermost nodes, the heat flow can be divided into two portions, one for each node, using current division method (Bird 2007). Take the thermal network from Figure 10 for demonstration. The

oscillatory response from source heat $_{sc}\tilde{p}_{i,h}$ into node 0 will be

$$_{sc\_0}^{1}\tilde{p}_{i,h} = \frac{^{scN \leftarrow N}t12_h}{^{1 \leftarrow N}t12_h} \cdot {_{sc}\tilde{p}_{i,h}} \tag{12}$$

where $scN \leftarrow N$ indicates the assembly consists of layers from scN (to the right of source node) to N.